DIFFUSION TENSOR IMAGING IN SEVEN MINUTES: DETERMINING TRADE-OFFS BETWEEN SPATIAL AND DIRECTIONAL RESOLUTION

Neda Jahanshad[1], Liang Zhan[1], Matt A. Bernstein[2], Bret J. Borowski[2], Clifford R. Jack Jr[2], Arthur W. Toga[1], Paul M. Thompson[1]

[1]Laboratory of Neuro Imaging, Dept. of Neurology, UCLA School of Medicine, Los Angeles, CA, USA
[2]Mayo Clinic, Rochester, MN, USA

ABSTRACT

Imaging protocols must obtain maximum information under tight time constraints, to minimize patient discomfort or attrition, and motion artifacts. As part of a pilot study optimizing DTI sequences for the Alzheimer's Disease Neuroimaging Initiative, we scanned 8 subjects with 3 DTI protocols of equal duration at two time-points (48 scans). If scan duration is fixed, collecting more diffusion-sensitized gradient directions can increase angular resolution at the expense of spatial. We compared 7-minute sequences with 3.0(48), 2.7(41), and 2.5(37) mm isotropic voxels (directions), to assess (1) SNR; (2) bias in estimating fiber anisotropy; (3) reproducibility over time; (4) intersubject variance--relevant for group comparisons. Statistical maps revealed that higher angular resolutions gave more reproducible estimates; FA depended on voxel size, with a steeper dependency in more heterogeneous regions. The intermediate resolution gave best SNR. 2mm DTI scans are common, but improved angular resolution may add temporal stability, and benefits for tractography.

Index Terms— Diffusion Tensor Imaging (DTI), spatial resolution, angular resolution, signal to noise, imaging protocols

1. INTRODUCTION

For all clinical applications, minimizing patient discomfort is vital. In non-invasive imaging, this mainly involves reducing the scan time as far as possible. Diffusion tensor imaging (DTI) is an MRI-based method to study water diffusion in tissue, and is particularly sensitive to neuronal myelination and white matter micro-architecture. It can also be used to study fiber connectivity in the brain. Various measures, most commonly fractional anisotropy (FA) and mean diffusivity (MD), may be computed from the local diffusion tensor. FA is often used as a measure of local fiber integrity, is correlated with cognitive performance [1], and is sensitive to brain maturation during development and degenerative processes in old age.

The diffusive properties of the anatomy are often modeled by tensors computed at every voxel [2]. Each diffusion tensor is mathematically represented by a 3x3 symmetric positive definite matrix, and may be visualized as an ellipsoid in space with varying levels of anisotropy. To estimate the elliptical tensors for DTI, at least 7 images are required, one with no diffusion sensitization, and 6 non-collinear gradient-encoded diffusion-weighted (DW) images. Due to the poor signal-to-noise in these images, it is often desirable to increase the angular resolution and obtain more than the minimal 7 images. SNR improvements level off as more gradient directions are collected, and SNR plateaus at different rates for different tensor-derived measures [3]. With more gradient directions, or more *q*-space samples at multiple *b*-values [4], one can calculate measures with greater angular and/or radial resolution, including the orientation distribution function (ODF) [5,6], the tensor distribution function (TDF) [7], or the full 3D diffusion propagator, to better characterize the fiber mixture in each voxel. Each DWI obtained takes a fixed amount of time, which depends on the protocol. The more refined the imaging grid, the longer the scan will take. Therefore, to increase the number of diffusion directions while maintaining scan time requires imaging on a coarser anatomical grid. It is therefore clinically useful to understand how trade-offs between angular and spatial resolution impact SNR, bias, and reproducibility, to use the available scan time efficiently.

Previous studies proposed optimal encoding schemes and *q*-space sampling strategies for diffusion tensor images. Many examined effects of applying different sets of gradients directions on diffusion measures [8,9] while others examined effects of spatial resolution [10]. Using 2 mm voxels at 4 Tesla, we recently found that SNR for FA and MD was near-maximal with 66 and 58 gradient directions, but for some ODF-derived measures, such as generalized fractional anisotropy (GFA), SNR still increased rapidly with even more gradient directions [3].

To the best of our knowledge, no study has evaluated the relative benefits of directional versus spatial resolution for ensuring that brain DTI measures are stable over time, given fixed scan time constraints.

Many studies describe procedures to boost SNR through lengthy imaging sessions or repeated scans that may be of value for research purposes [11]. However, long scans

can be impractical when imaging children or subjects who are ill or elderly, especially in longitudinal studies where the added patient burden will lead to sample attrition. Methods to minimize noise have been proposed [12]. These procedures may also benefit from estimates of the reproducibility of various acquisitions.

Approaches have also been proposed to optimize the gradient encoding scheme depending on the orientation of the fibers of interest [13] by applying magnetic field gradients to particular locations around the unit sphere rather distributing them uniformly. However, this method may be problematic if the goal is to examine fiber orientations throughout the brain without bias.

Here we imaged eight subjects with three different scanning protocols at two separate time-points. Our goal was to determine the longitudinal reproducibility, SNR, cross-subject variance, and biases, for clinically relevant DTI-derived features. We hope our efforts will help medical researchers decide among protocols when making trade-offs to stay within time constraints.

2. METHODS

2.1. Image Acquisition

We acquired diffusion tensor (DT) MRI scans from 8 subjects (age: 32.0 +/- 3.9SD; 4 male, 7 right handed) using a GE 3T MRI scanner running 14.0 M5 software. To explore the trade-off between spatial and angular resolution, we used three separate acquisition protocols, each with the acquisition time held fixed at 7 min +/- 3 sec. For each series of images, there was an additional EPI calibration scan lasting approximately 1 min.

Contiguous axial slices were obtained with b = 1000 s/mm^2. To ensure whole-brain coverage, the field of view was fixed at 119 ± 1 mm in the S/I direction and 230.0 ± 0.4 mm A/P. The coverage in the R/L direction (i.e., the frequency encoded direction) exceeded 320 mm in all cases, so it easily covered the entire head. All imaging protocols acquired 4 b0 images, i.e., T2-weighted images without diffusion sensitization. To keep scan time fixed, TR was allowed to vary, as was the number of DTI angular gradient directions. The acquisition parameters are summarized in **Table 1.**

	R1	***R2***	***R3***
Isotropic (mm)	**3.0**	**2.7**	**2.5**
DTI gradient dirs.	**48**	**41**	**37**
TR (ms)	7750	9000	9825
Number of slices	40	44	48
FOV -S/I (mm)	120	118.8	120
FOV-A/P (mm)	230.4	230.1	230.4
FOV-R/L (mm)	384	350	320

Table 1: Different parameters used for each protocol.

Throughout this paper we will refer to these three resolutions by their isotropic voxel size. Each subject was imaged on two separate occasions, two weeks apart, with each protocol.

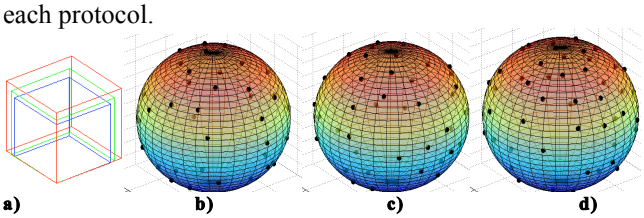

Figure 1: a): Three different voxel sizes were used. The smallest (blue cube) voxel size (2.5 mm width) corresponds to the protocol with the *lowest* number of gradient directions. (**b-d)** show points on the unit sphere where diffusion-sensitized gradients were applied for each protocol; the number of gradient directions increases from left to right: 37 in (b), 41 in (c), and 48 in (d).

2.2. Preprocessing, Registration and Tensor Estimation

For all 48 sets of images (8 subjects, 3 protocols, 2 time points), diffusion-weighted images were corrected for motion and eddy current distortion using the 'eddy_correct' command from the FSL toolbox (http://fsl.fmrib.ox.ac.uk/fsl) to align all images in the volume to the first image without diffusion sensitization (b0). The resulting set of images was then used to calculate diffusion tensors using MedINRIA software (http://www-sop.inria.fr/asclepios/software/MedINRIA). Extra-cerebral matter was removed from the images using the 'bet' tool from FSL.

The first b0 image of all subjects, which was used as the reference image for motion and eddy current correction, was aligned to a common template. All subjects' images were linearly registered to a high-resolution single subject average scan, the Colin27 [14], using FLIRT software (http://fsl.fmrib.ox.ac.uk/fsl/flirt) with 9-parameter (df) registration – to avoid shearing - and a mutual information cost function. The corresponding transformation matrices were retained. To optimize registration, these linearly aligned images were then mapped to the template using a mutual information based elastic registration [15].

2.3. Anisotropy and Signal to Noise (SNR) Calculations

Linearly aligned tensors were used to obtain scalar maps of anisotropy. Eigen-values were extracted from the diffusion tensors and common measures of anisotropy - fractional anisotropy (FA), and the mean diffusivity (MD) - were calculated as follows:

$$FA = \sqrt{\frac{3}{2}} \frac{\sqrt{(\lambda_1 - \bar{\lambda})^2 + (\lambda_2 - \bar{\lambda})^2 + (\lambda_3 - \bar{\lambda})^2}}{\sqrt{\lambda_1^2 + \lambda_3^2 + \lambda_3^2}}$$

$$MD = \bar{\lambda} = \frac{\lambda_1 + \lambda_3 + \lambda_3}{3}$$

Once these scalar maps were calculated, the corresponding deformation fields from the nonlinear mappings were applied to align anatomy across protocols.

Signal-to-noise ratio (SNR) is reported as a ratio between the mean signal for all subjects over the standard deviation, in regions of interest selected for their anatomical homogeneity.

2.4. ROI Extraction and Statistical Analyses

To compare anisotropy measures in the subjects' anatomy across protocols, regions of interest (ROIs) were manually extracted from the template scan and applied to the individual registered scans. Regions examined included the splenium of the corpus callosum, and the frontal lobe.

For statistical analyses, we used paired Student's *t*-tests to compare ROI and voxel-based anisotropy measures across time points and to compare various scanning protocols. As we expected noise to play a role in this analysis, we also examined protocol-dependent differences in the group variance of FA and MD values, using *F*-tests.

3. RESULTS

3.1. Anisotropy Averages

Figure 2 shows the mean and standard deviations for the FA and MD measures, for each scanning protocol (N=16). Qualitative differences are seen among the three different protocols.

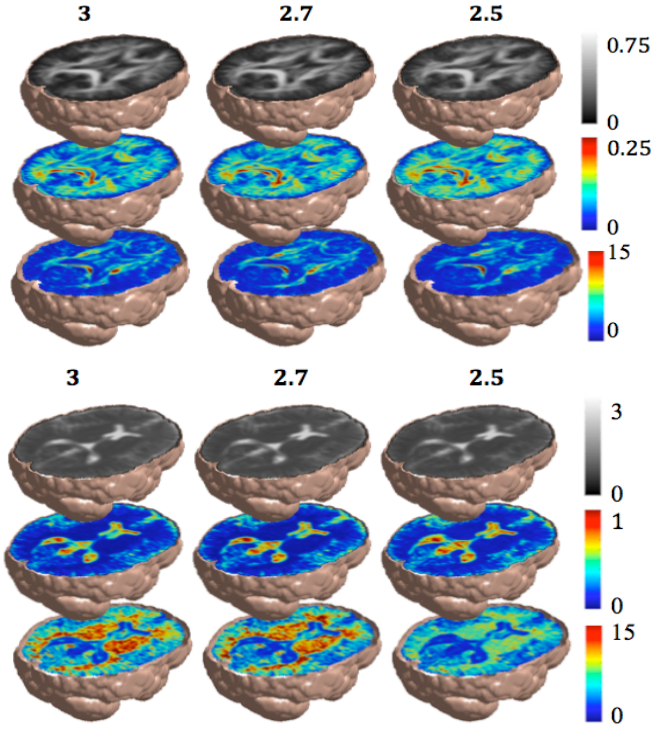

Figure 2: The means (top), stddev (mid), and SNR = mean/stddev (bottom) for FA (**a**) and MD (**b**) are shown for all resolutions. 2.5mm scans give higher variance in caudate and optic radiations, resulting in a lower SNR.

3.2. Differences in Anisotropy Mean and Variance

Figure 3 shows significant differences in FA and MD values between the three different resolutions using one sided paired t-tests including every subject at a single time point (N=8). False Discovery Rate (FDR) analysis confirmed these differences after multiple comparison correction.

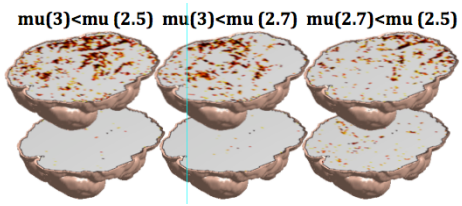

Figure 3: One-sided pairwise *t*-tests, comparing FA between protocols, highlight regions where the coarser spatial resolution image had systematically lower anisotropy—this is due a greater partial volume effect. No significant differences were detected for MD maps (*bottom*).

Figure 4 highlights regions where the group variance between the resolutions is significantly different, using one sided paired *F*-tests at every voxel. In general, sequences with large voxels and more gradient directions have less noise and variance across the subject sample.

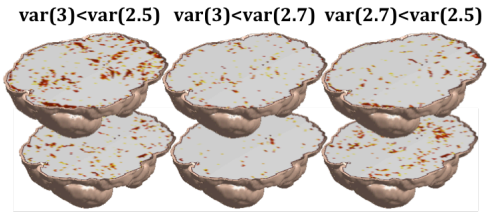

Figure 4: *F*-tests at every voxel highlight differences in sample (cross-subject) variances between protocols for FA (top) and MD (bottom). No significant difference is seen between 3mm and 2.7mm voxels. The 2.5mm protocol gives higher variance across the sample.

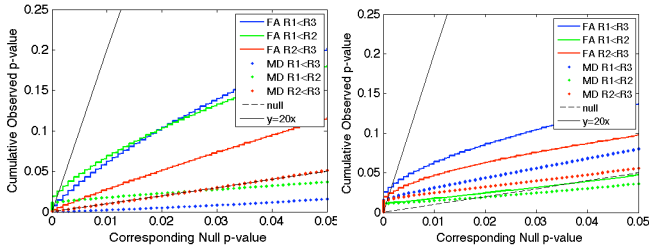

Figure 5: Multiple comparison correction was performed using the false discovery rate procedure for *t*-tests (left) and *F*-tests (right). Significant differences exist in the means and variance of anisotropy for voxels of size 2.5 and 3mm.

3.3. ROI analysis and Consistency

Figure 5 shows average FA values in the frontal lobe and splenium, plotted against the number of gradient directions.

The average FA values in the ROIs were also measured at each time-point. The protocol using 3mm isotropic voxels was most stable over time, but it gave artificially lower

values for FA (**Figure 8**); this is a known consequence of increased partial volume effects, in which voxels with more than one fiber direction appear more isotropic when large voxels are used.

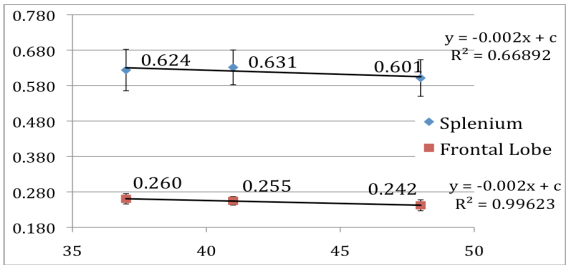

Figure 6: Mean FA values are shown (error bars denote standard deviations) for ROIs using various scan resolutions. Higher linear correlations with voxel size are found in the frontal lobe, which has more fiber crossing (partial volumed voxels) than the splenium. As expected, effects of voxel size on FA are less pronounced in regions where fiber coherence is high.

Figure 7 shows the average (*N*=8) absolute difference, and standard deviation of differences, between time points for FA at every resolution.

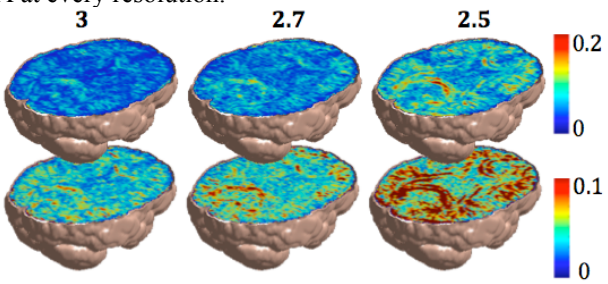

Figure 7: Maps of mean and standard deviation for the absolute FA difference in scans across time. Scans with larger voxels, but more gradient directions, give more reproducible measures. This stability is important for longitudinal studies.

4. CONCLUSIONS

Differences were clear between the two most extreme resolution protocols (3mm versus 2.5mm voxels). Scans with the largest voxel size and angular resolution were most stable over time, and had least variance for DTI-derived measures across the group of 8 subjects. Scans with smaller voxels and sparser angular sampling were less stable over time. The intermediate resolution scan had highest SNR, and intermediate stability and bias for FA estimation.

In future, we will examine specific tracts and compare images after DTI denoising and other types of cross-subject registration. We will also examine uncertainty in the principal eigenvector field, and in the directions of the ODF maxima, to understand how these protocols may affect reconstruction accuracy in tractography studies.

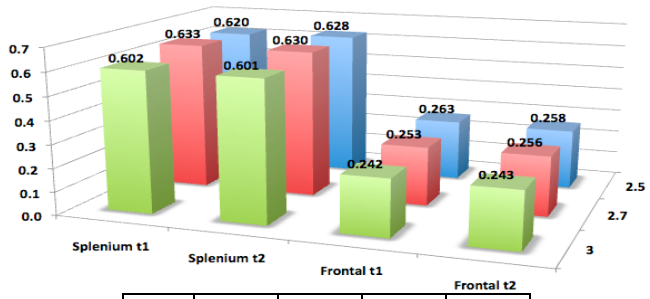

SNR	S t1	S t2	F t1	F t2
2.5	11.48	9.97	17.54	18.41
2.7	13.76	12.11	19.48	23.31
3	12.04	11.33	17.28	14.28

Figure 8: FA in the splenium and the frontal lobe plotted at 2 time points, t1 and t2. SNR (μ/σ), is consistently highest in the scans with intermediate voxel size (*middle row*).

5. REFERENCES

[1] Chiang MC et al. Genetics of brain fiber architecture and intelligence. **J. Neuroscience**, Feb 18; 29(7):2212-24 (2009)

[2] Basser P et al. Estimation of the effective self-diffusion tensor from the NMR spin echo. **J Mag Res B** 103, 247-254 (1994)

[3] Zhan L et al. How does angular resolution affect diffusion imaging measures? **NeuroImage**, available online Sep. 2009, DOI: 10.1016/j.neuroimage.2009.09.057 (2009)

[4] Wedeen VJ et al. Mapping complex tissue architecture with diffusion spectrum magnetic resonance imaging, **MRM** 54(6):1377-1386 (2005)

[5] Tuch DS. Q-ball Imaging. **MRM** 52(6):1358-1372 (2004)

[6] Aganj I. ODF reconstruction in *q*-ball imaging with solid angle considerations. **Proc. IEEE ISBI** (2009)

[7] Leow AD et al. The tensor distribution function. **MRM** 61(1):205-214 (2008)

[8] Landman B et al. Effects of diffusion weighting schemes on the reproducibility of DTI-derived fractional anisotropy, mean diffusivity, and principal eigenvector measurements at 1.5T, **NeuroImage** 36(4): 1123-1138 (2007)

[9] Hasan KM et al. Comparison of Optimization Procedures for Diffusion Tensor Encoding Directions **Proc ISMRM** 8:792 (2000)

[10] Fujiwara S et al. Feasibility of 1.6mm isotropic voxel diffusion tensor tractography in depicting limbic fibers. **Diagnostic Neuroradiology** 50:131-136 (2008)

[11] Liu X et al. Optimization of in vivo high-resolution DTI of non-human primates on a 3T human scanner. **Methods** (2009)

[12] Hasan KM et al. Evaluation of SNR Performance and Utility of High Spatial and Angular Resolution Denoised 1mm^3 Isotropic DTI of Entire Human Brain at 3T. **Proc ISMRM** 14:334 (2006)

[13] Peng H, Arfanakis K. Diffusion tensor encoding schemes optimized for white matter fibers with selected orientations. **Mag Res Imaging** 25:147:153 (2007)

[14] Holmes CJ et al. Enhancement of MR images using registration for signal averaging. **JCAT** 22(2):324-33 (1998).

[15] Leow A et al. Statistical Properties of Jacobian Maps and the Realization of Unbiased Large-Deformation Nonlinear Image Registration, **IEEE TMI** 26(6):822-832(2007)